5-1-2023

Cycle Time Reduction in Additive Manufacturing using Peltier Thermoelectric Cooling Devices

Trevor Carlton
Georgia Southern University

Cycle Time Reduction in Additive Manufacturing using Peltier Thermoelectric Cooling Devices

An Honors Thesis submitted in partial fulfillment of the requirements for
Honors in Mechanical Engineering

By
Trevor Carlton

Under the mentorship of Dr. David Calamas

ABSTRACT

Thermoelectric cooling and the Peltier effect were discovered in 1834, over 188 years ago. Additionally, the first iterations of additive manufacturing (i.e., 3D printing) began in the early 1980s, more than 40 years ago. Despite these technologies' age and years of advancements, the application of Peltier cooling-based devices in additive manufacturing has not yet been realized. These devices can be used for the active thermal management of print beds in 3D printers. Developing a mechanism to heat and cool a print bed can reduce the cycle time to manufacture a part. In 3D printing, waiting for the heated bed to cool down before removing the part due to potential deformations and loss of finishing quality is best. Removing the part before the printer bed cools down can damage the print bed surface. Due to this time constraint, the automation and mass production of 3D-printed parts is substantially hindered. Using a thermoelectric cooling device, known as a Peltier cooler, a 3D printer bed could be cooled using the Peltier and Seebeck Effects by applying a voltage to the device. Furthermore, the Peltier cooler could serve as a dual-purpose device to heat the printer bed to the desired temperature. The result is a decrease in the total time to manufacture multiple parts additively.

Thesis Mentor: _____
Dr. David Calamas

Honors Director: _____
Dr. Steven Engel

May 2023

Department of Mechanical Engineering

University Honors Program

Georgia Southern University

Acknowledgments

I would like to thank my faculty advisor, Dr. David Calamas, for his guidance and support throughout this project. I appreciate the time and effort he has invested in this project, and I am grateful for the opportunity to work under his supervision.

I would also like to extend my thanks to the Mechanical Engineering Department and the University Honors Program for providing me with the necessary resources, knowledge, and equipment to conduct this research.

I wish to express my gratitude to my friends who have been there for me throughout this journey. Ana Abadie, Matthew Adharsingh, Kiera Ferrell, Andrew Joiner, Kody Pierce, Cameron Stuart, and Garrett Sydnor have been great friends and have provided me with support and encouragement throughout my college experience. I appreciate all that they have done for me, and I am grateful for their friendship.

Lastly, I want to express my heartfelt appreciation and gratitude to all my family for their unwavering support and guidance. None of this would have been possible without them. My mom and dad, JohnTyler, Grannie, and Callie have been there for me every step of the way, providing me with their guidance, wisdom, and encouragement. Their love and support have been invaluable. I am truly blessed to have such an amazing family, and I am forever grateful for their impact on my life.

Table of Contents

List of Figures

List of Tables

1. Introduction

1.1 Background and Motivation

Additive manufacturing is a rapidly growing field and is starting to have a significant role in industrial and commercial industries. “3D printing technology has the [probability] to revolutionize industry and production processes. Fabrication will be low while costs are reduced thanks to 3D printing technology” [1]. There are advantages to additive manufacturing, such as rapid prototyping, the ability to create complex geometries, and low manufacturing cost. However, some disadvantages and drawbacks must be addressed, such as “Part size limitations, elephant foot…warping, poor accuracy, [and] low manufacturing efficiency” [1]. As this field expands, so does the demand for an automated additive manufacturing process that can produce mass-produced components. Increasing manufacturing efficiency is a crucial element for the mass production of components. Phillips [6] wrote about the slow fabrication speeds of additive manufacturing relative to other manufacturing techniques. Additionally, it was shown by Glatt, Greco, Yi, Kirsch, and Aurich [2] that the manual removal of finished parts from the print bed reduces the overall productivity of the process, and they were able to successfully develop a system for automated removal of FDM 3D printed parts. However, there is still room for improvement in the overall efficiency of automated processes. In 3D printing, waiting for the heated bed to cool down before removing the part due to potential deformations and loss of finishing quality is best. Removing the part before the printer bed has cooled down can also damage the print bed surface. Implementing a system that rapidly cools the print bed could reduce the overall cycle time of a part and increase manufacturing efficiency.

1.2 Objectives

The primary objective of this project is to explore and experimentally test a novel idea for an active cooling system for a 3D print bed. The active cooling system for the print bed will utilize Peltier thermoelectric devices in place of the traditional resistance heating element currently used in virtually all existing heated 3D printer beds. Each method's heating and cooling uniformity and cycle time will be evaluated and compared to determine if this active cooling system is viable to increase manufacturing efficiency in automated processes.

1.3 Peltier Thermoelectric Coolers

Using a thermoelectric cooling device known as a Peltier cooler or TEC, a 3D printing bed could be cooled rapidly by applying a voltage to the device. This device acts as a solid-state heat pump and operates using the Peltier and Seebeck Effects [3-5]. The Peltier effect operates by directing current through a pair of dissimilar metals. The current loop comprises several semiconductor electrode pairs, "the current at the cold side flows from n-type semiconductor to p-type semiconductor, the temperature at the cold side drops, and it absorbs heat from the heat source" [5]. The configuration of a TEC, including the p-type and n-type semicondutors, can be found in Figure 1.

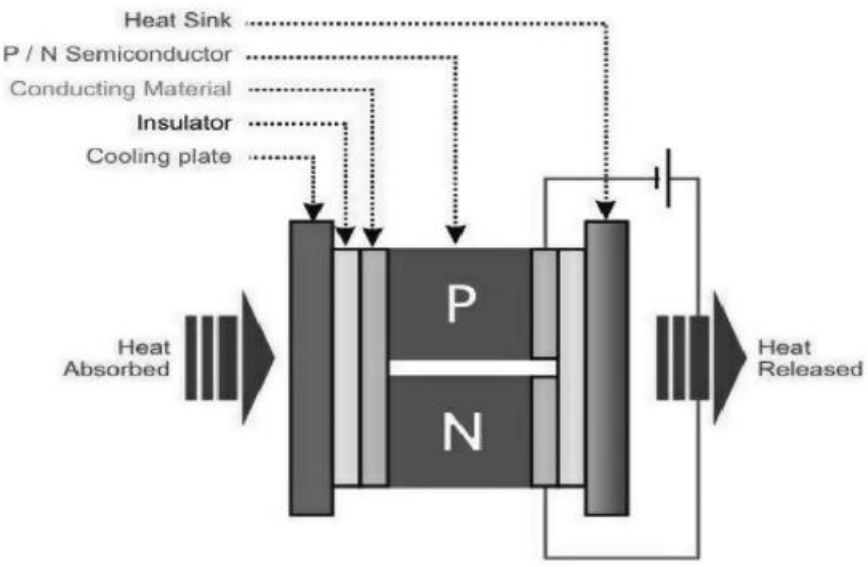

Figure 1: Thermoelectric Cooler Configuration

The type of thermoplastic being used to print is a factor to consider when assessing the Peltier cooler's effectiveness in cooling. Depending on the material of the filament being printed, the required print bed temperature varies from as low as 50 to as high as 110 degrees Celsius [7]. This project will focus on Polylactic acid (PLA) type thermoplastic, which is not recommended to exceed any print bed temperature above 70°C. "Directly after printing, a non-destructive removal of the printed part may not be attainable at [high] bed temperature[s]" [8]. Spoerk, Gonzalez-Gutierrez, Sapkota, Schuschnigg, and Holzer acknowledge the need to reduce the bed temperature before removal of the part and state, "if the occurrence of welding can be precluded, it may be favorable in this regard to cool the printing bed first to a certain temperature, at which the adhesion forces are sufficiently reduced" [8]. Furthermore, the Peltier cooler could serve as a dual-purpose device to heat the printer bed to the desired temperature. Heating the print bed can be achieved by

reversing the current direction, which would reverse the direction of heat transfer, causing heat to be displaced on the side of the device connected to the print bed.

1.4 Heat sinks

Heat sinks play an essential role in the performance of a thermoelectric cooler. TECs transfer heat well but do not dissipate heat well, and damage can occur if no dissipation is allowed [12,13]. A heat sink placed on the hot side of a TEC will allow for greater heat dissipation and overall performance of the module [9,10]. Xia, Zhao, Zhang, Yang, Feng, Zhang, and Song conducted a study on the performance of TECs with varied finned heat sink configurations and stated, "improving heat dissipation conditions can improve the cooling performance of thermoelectric cooling units and the system's COP value," and heat dissipation should be prioritized [10]. The study found that a sub-plate finned heat sink produced the best heat dissipation, and the cooling capacity could be increased by 70% compared to non-optimized commercial TECs [10]. Additionally, a study conducted by Abbas and Wang [11] found that by integrating a fin displacement design, the maximum reduction in thermal resistance was 56% and a 27.8% total mass reduction compared to traditional heat sinks. Therefore, implementing specialized heat sinks would significantly increase the efficiency and effectiveness of rapidly cooling a print bed.

2. Experimental Methodology

The heating and cooling of a 3D printer bed will be experimentally tested by implementing a Peltier cooler array and be compared to the traditional method of resistance heating natural convection. A Creality Ender 3 3D printer with a print bed size of 235 mm by 235 mm was used to collect heating and cooling data with the traditional resistance

heating element. The print bed was heated from 24 °C to 70 °C using the resistance heating element on the underside of the print bed installed by the manufacturer. The resistance heating element was then turned off to allow natural convection to cool the print bed back to 24 °C. A FLIR A300-Series camera and its companion software ResearchIR were used to record the print bed's minimum, average, and maximum surface temperature during the heating and cooling process. Ten trials each were conducted for the heating and cooling process. Each heating and cooling trial using this method lasted approximately 4 minutes and 30 minutes, respectively.

Figure 2: Resistance Heating Element Experimental Setup

A 235 mm by 235 mm by 4.8 mm 6061-T6 aluminum plate was used as a print bed surface to construct the Peltier cooling system. The Peltier thermoelectric cooler modules utilized in the experiment are TEC 12706. An evenly distributed 3×3 grid of the TEC 12706 modules were constructed on the underside of the aluminum plate and fastened using thermal glue. In addition, 40 mm by 40 mm by 5 mm aluminum heat sinks were fastened using thermal glue on the opposite-facing side of each Peltier cooler to allow for more heat dissipation.

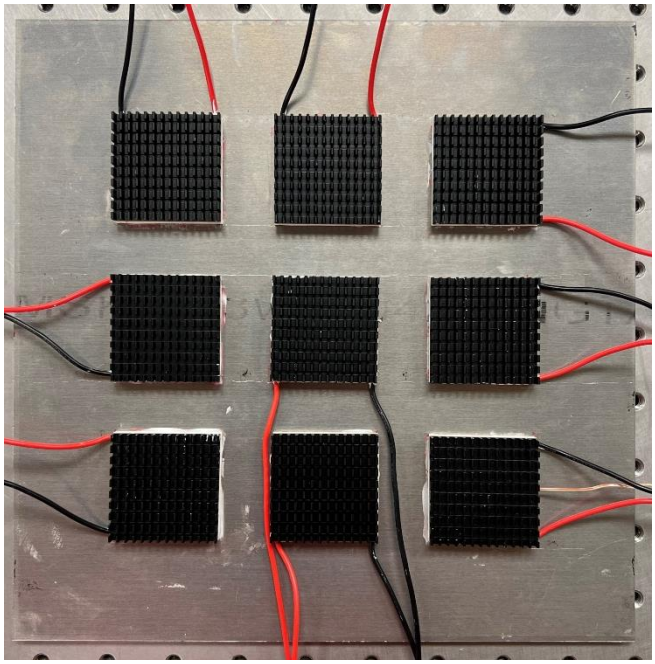

Figure 3: Peltier Device 3x3 Grid Setup

Additionally, a K-type thermocouple was mounted between one of the heat sinks and Peltier surfaces and connected to an Omega CSC32 Benchtop Temperature Controller to monitor the device's temperature. This was done to ensure the device did not exceed the maximum operating temperature of 120 °C, as stated in the TEC 12706 module

specification sheet. The circuit was constructed such that each row was connected in series, and each column was connected in parallel. The BK Precision 1735A DC bench power supply was used to power the circuit of Peltier coolers and only could supply a maximum current of 3A. The Peltier coolers will not be powered to their maximum capacity as the TEC 12706 module can be supplied up to 6A. The circuit was powered and allowed to heat the print bed from 24 °C to 70 °C. Once the print bed reached 70 °C, the current direction through the circuit was reversed to change the direction of heat transfer through the Peltier devices. The Peltier devices were powered in this state until the maximum operating temperature of 120 °C on the hot side was reached. The Peltier coolers remained powered off, and natural convection was resumed until the print bed returned to a temperature of 24 °C. The FLIR A300-Series camera was again used during the heating and cooling processes to record the print bed's minimum, average, and maximum surface temperature. Ten trials each were conducted for the heating and cooling process.

Figure 4: Peltier Heating and Cooling Experimental Setup

Each heating and cooling trial using this method lasted approximately 15 and 35 minutes, respectively. Duration and uniformity comparisons between the two methods were made once the data was collected and analyzed.

3. Data / Calculations

3.1 Data

Each trial was conducted with an approximate ambient temperature of 24 °C, and can be found in Table 1 through Table 4. ΔT is the temperature difference between the maximum and minimum temperatures and represents the uniformity of the heating and cooling processes.

Table 1: Resistance Heating Element Average Temperature

Resistance Heating Element Average Temperature				
Time (Minutes)	Minimum Temperature (°C)	Average Temperature (°C)	Maximum Temperature (°C)	ΔT (°C)
0	23.07	23.50	23.87	0.80
1	30.86	38.49	41.79	10.92
2	43.88	54.77	59.75	15.87
3	54.96	66.13	71.41	16.44
4	58.11	66.70	70.47	12.35

Table 2: Natural Convection Cooling Average Temperature

Natural Convection Cooling Average Temperature				
Time (Minutes)	Minimum Temperature (°C)	Average Temperature (°C)	Maximum Temperature (°C)	ΔT (°C)
0	60.45	67.30	70.34	9.89
5	49.68	52.66	54.10	4.42
10	41.85	43.81	44.82	2.97
15	36.95	38.39	39.20	2.25
20	33.76	34.85	35.51	1.75
25	31.48	32.38	32.96	1.49
30	29.76	30.61	31.18	1.42

Table 3: Peltier Heating Average Temperature

Peltier Heating Average Temperature				
Time (Minutes)	Minimum Temperature (°C)	Average Temperature (°C)	Maximum Temperature (°C)	ΔT (°C)
0	24.01	24.63	25.09	1.08
1	24.67	30.05	33.66	8.98
2	27.18	34.66	38.13	10.94
3	30.43	38.63	42.12	11.69
4	33.73	42.12	45.69	11.96
5	36.97	45.29	48.95	11.98
6	40.57	48.16	51.92	11.35
7	43.59	50.88	54.81	11.22
8	45.98	53.45	57.50	11.52
9	47.81	55.74	59.84	12.03
10	49.65	57.85	62.03	12.38
11	51.02	59.77	63.99	12.97
12	52.63	61.56	66.19	13.56
13	53.95	63.22	67.80	13.86
14	55.03	64.68	69.51	14.48
15	56.22	66.02	71.13	14.91

Table 4: Peltier Cooling Average Temperature

Peltier Cooling Average Temperature				
Time (Minutes)	Minimum Temperature (°C)	Average Temperature (°C)	Maximum Temperature (°C)	ΔT (°C)
0	56.59	63.41	65.70	9.12
0.1	56.33	62.64	64.88	8.56
0.2	56.04	61.80	64.15	8.12
0.3	55.81	60.88	63.15	7.34
0.4	55.44	60.13	62.23	6.80
0.5	54.87	59.45	61.48	6.60
0.6	54.53	58.87	60.97	6.45
0.7	54.20	58.48	60.70	6.50
0.8	53.69	58.06	60.43	6.74
0.9	53.25	57.79	60.22	6.97
1.0	52.77	57.69	60.18	7.42
1.5	51.72	58.06	60.90	9.18
2.0	51.32	57.88	60.64	9.32
5.0	48.52	52.47	53.84	5.32
10.0	39.29	43.05	43.97	4.68
15.0	33.44	36.79	37.55	4.11
20.0	30.09	32.78	33.42	3.33
25.0	27.87	30.05	30.58	2.71
30.0	26.60	28.16	28.63	2.03

4. Results and Discussion

4.1 Initial Results

The average minimum and maximum temperatures and average temperature differences across the ten trials for each method were plotted and can be found in the figures below. In addition, screenshots of the temperature contours from the FLIR camera during the experimental trials can also be found in the figures below.

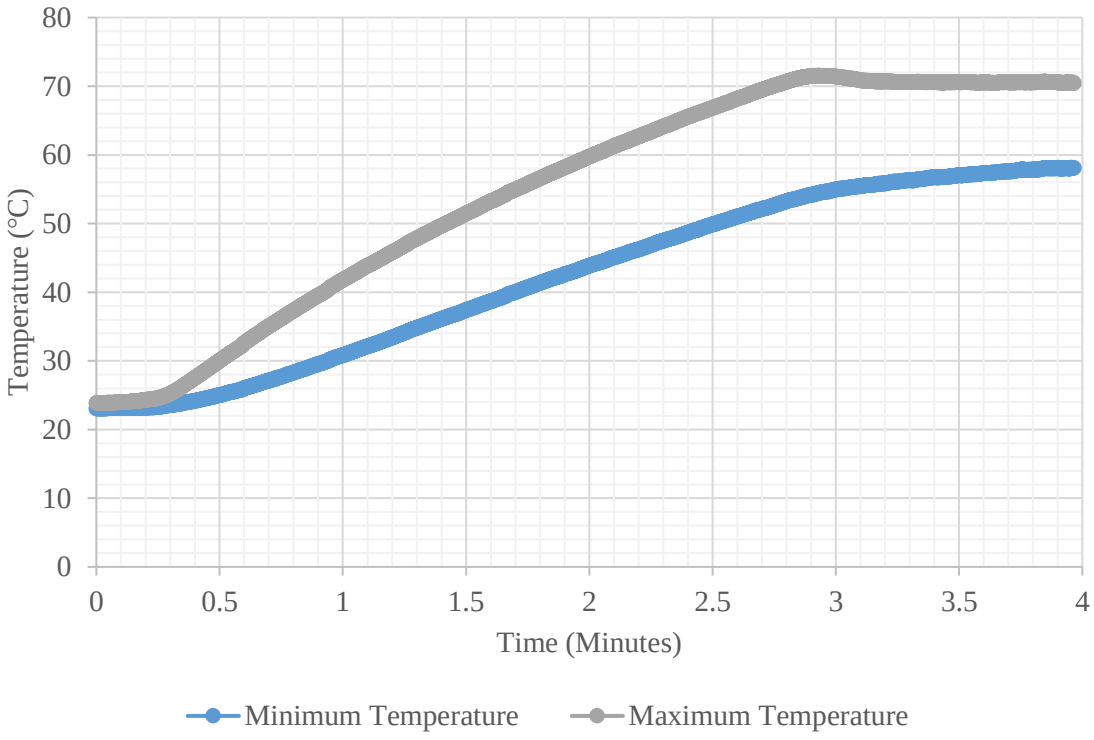

Figure 5: Resistance Heating Trials Average Temperatures

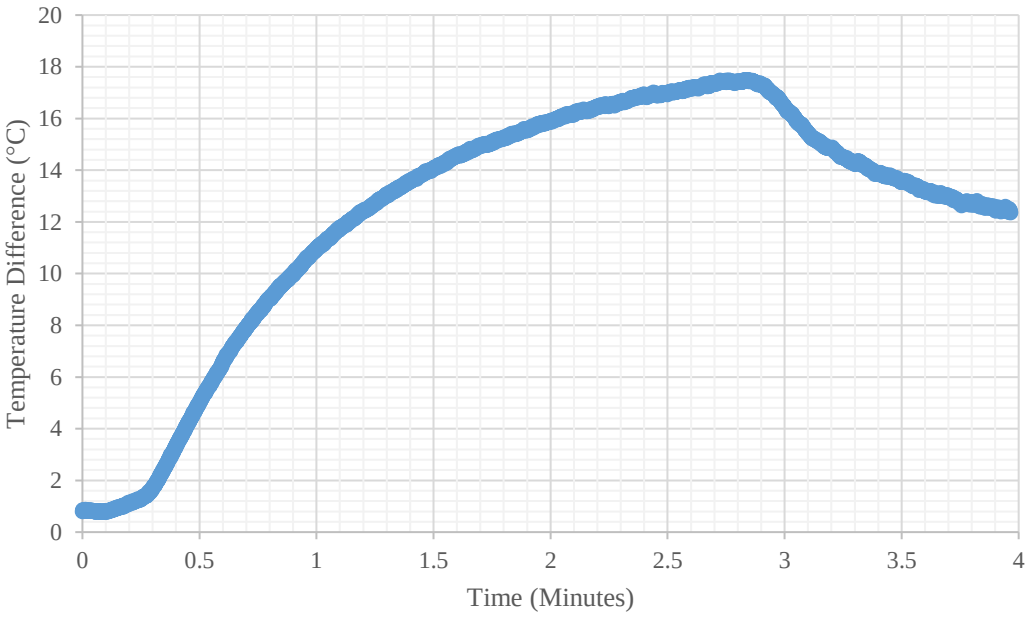

Figure 6: Resistance Heating Trials Average Temperature Difference

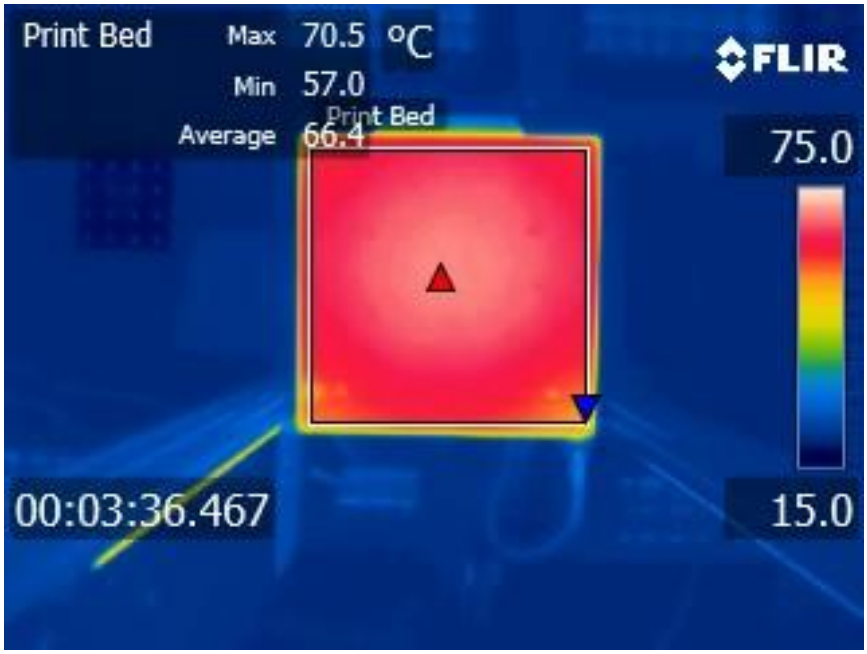

Figure 7: Resistance Heating Element FLIR Camera Snapshot

The resistance heating element heated the print bed in approximately 4 minutes on average, as seen in Figure 5. The ΔT represents the heating uniformity across the print bed throughout the trial. As shown in Figure 6, the temperature difference continually increases until minute 3 at a maximum ΔT of 17.43 °C, then decreases to 12.36 °C at minute 4. Resistance heating elements are exceptionally well at uniform heating. In Figure 7, the FLIR snapshot shows a very uniform print bed surface. The high temperature difference is likely due to the lower temperatures on the outer edges of the print bed, which this area does not play an essential role in the printing process. In the FLIR snapshot in Figure 7, this can be observed by the blue triangle marker, which indicates the coldest point in the defined area.

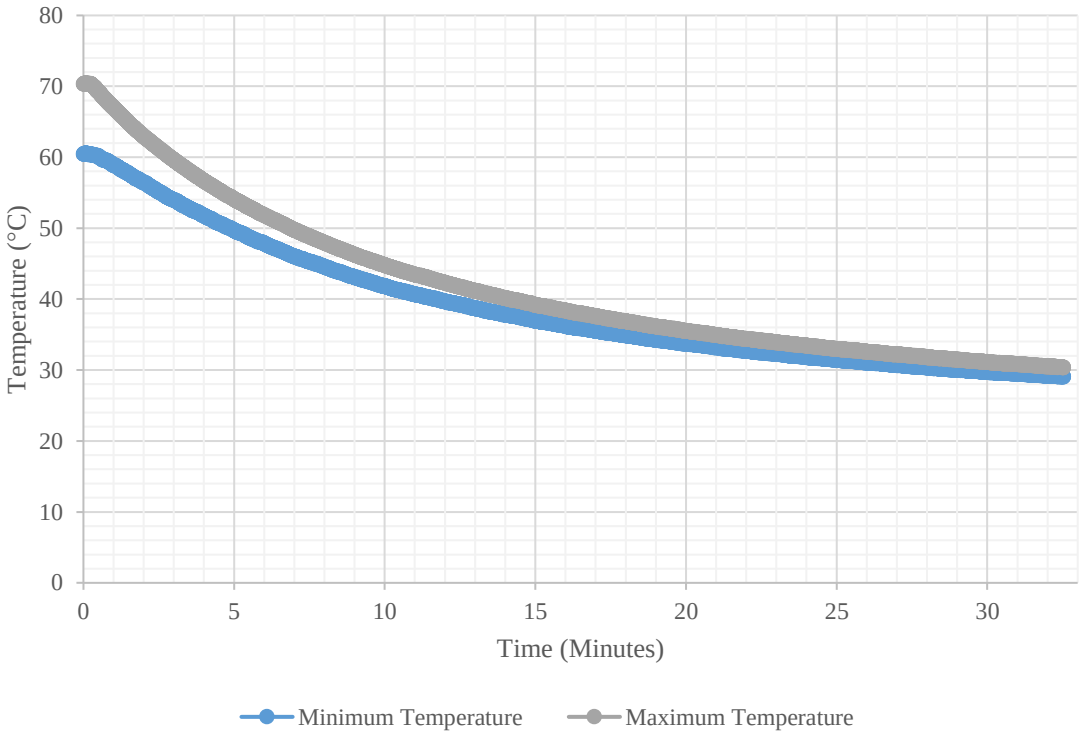

Figure 8: Natural Convection Cooling Trials Average Temperatures

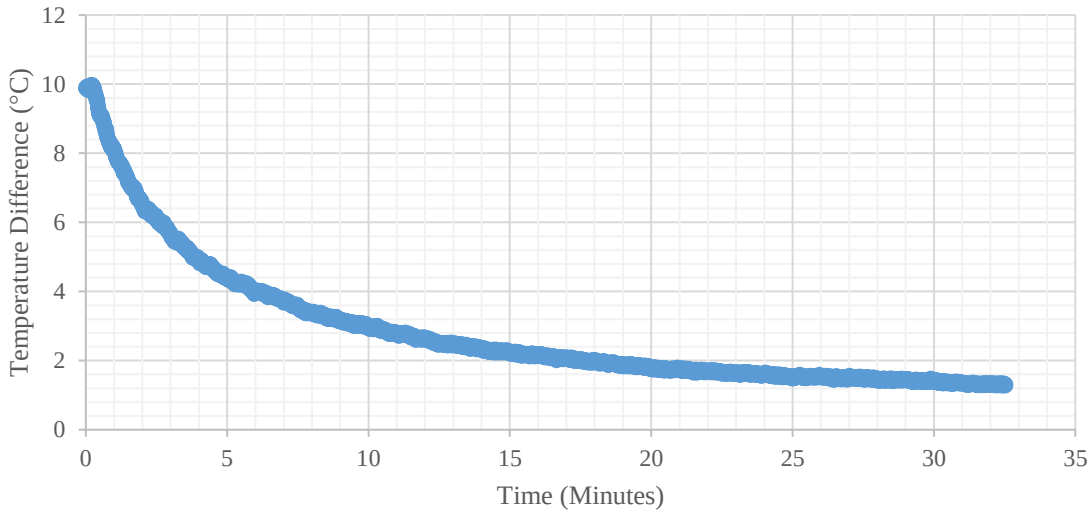

Figure 9: Natural Convection Cooling Trials Temperature Difference

Figure 10: Natural Convection FLIR Camera Snapshot

The natural convection duration to cool the print bed surface from 70 °C to 24 °C was 30 minutes on average, as shown in Figure 8. The temperature across the print surface, as it cools, is very uniform and can be seen in Figure 9 and Figure 10. Figure 9 shows the continual decrease in the temperature difference through the duration of the experimental trial. The high initial temperature difference is likely due to the same issue of the outer edge temperatures of the defined measurement area.

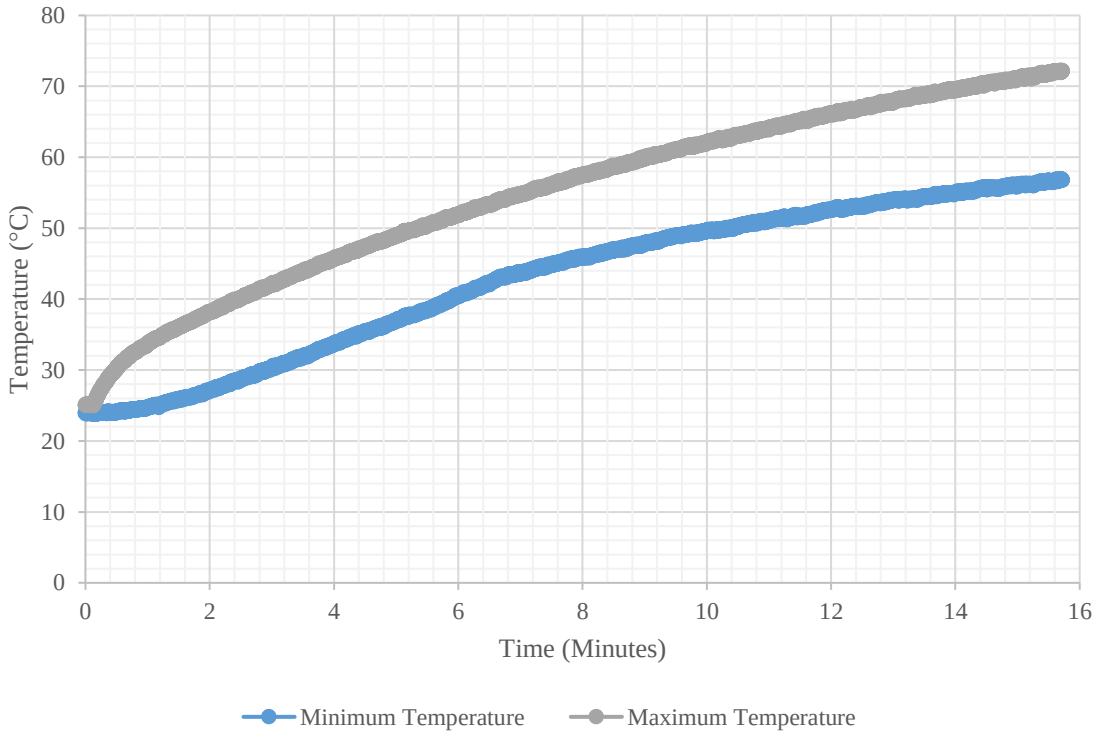

Figure 11: Peltier Heating Trials Average Temperatures

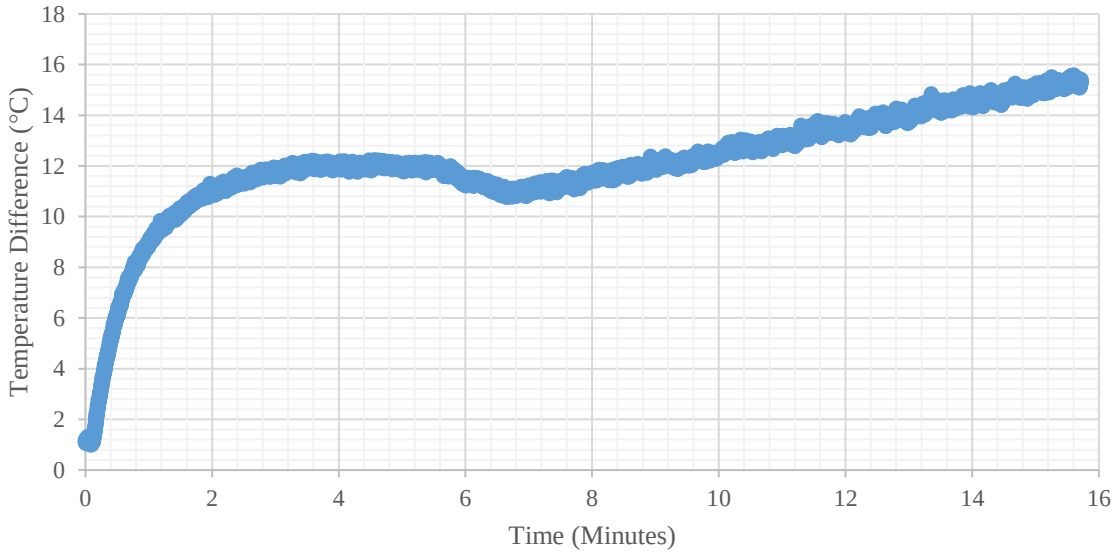

Figure 12: Peltier Heating Trials Average Temperature Difference

Figure 13: Peltier Heating FLIR Camera Snapshot

The Peltier devices heating the aluminum print bed from 24 °C to 70 °C had an average duration of 15.7 minutes, as shown in Figure 11. The temperature across the print surface was non-uniform, as shown in Figure 12. The temperature difference maintained a high value throughout the duration of the experiment. The non-uniform temperature can best be seen in The FLIR camera snapshot in Figure 13 and is due, in part, to the underperforming top row of Peltier devices. An internal defect in a Peltier device in that row is likely to be the cause for the row to underperform compared to the bottom two rows. The internal defect in a single Peltier device would affect the current flow through the entire row because of the series connections. The highest ΔT recorded in Figure 12 was 15.25°C at 15.7 minutes.

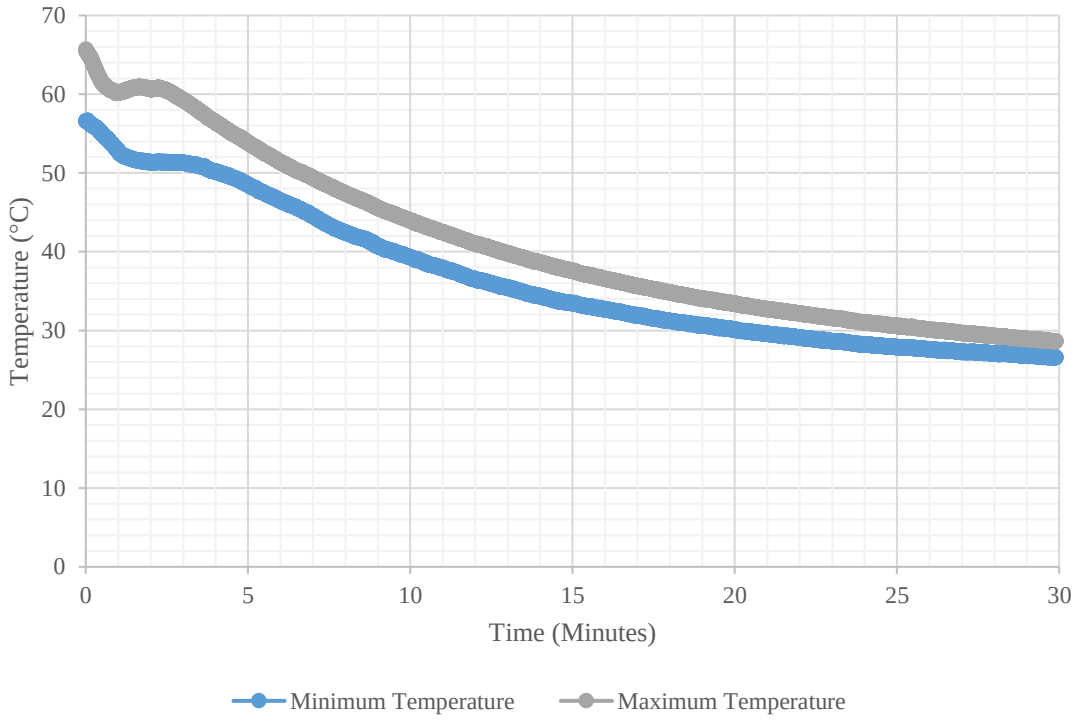

Figure 14: Peltier Cooling Trials Average Temperatures

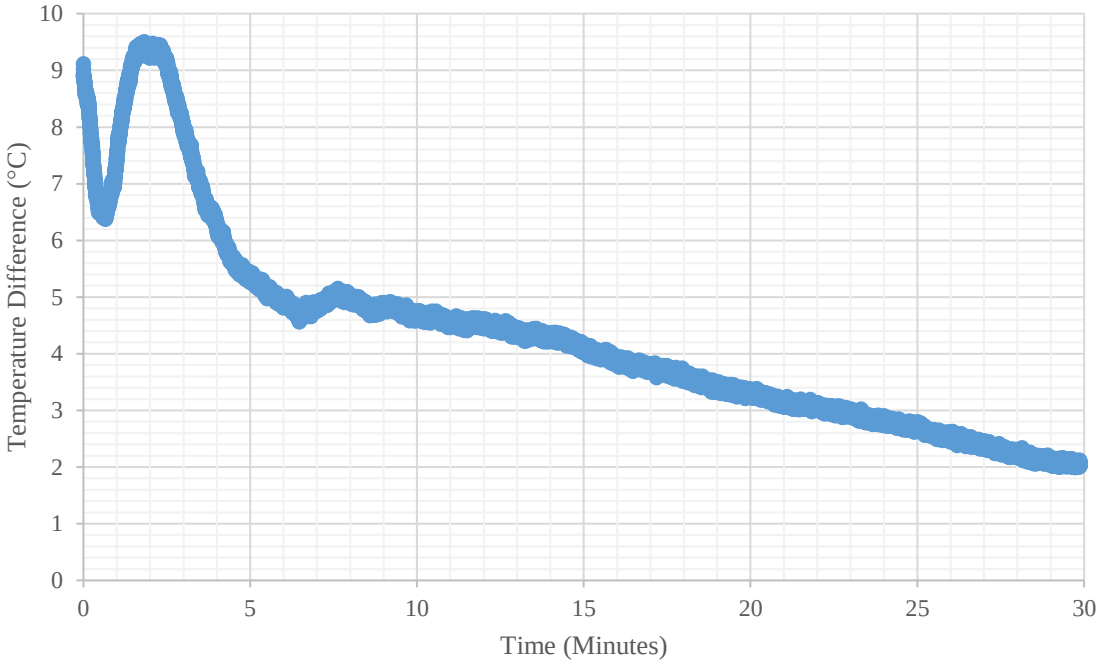

Figure 15: Peltier Cooling Trials Average Temperature Difference

Figure 16: Peltier Cooling FLIR Camera Snapshot

Figure 17: Peltier Cooling Heat Bleed FLIR Camera Snapshot

The print bed surface cooled from 70 °C to 24 °C in approximately 35 minutes on average during the Peltier cooling trials. The Peltier devices were not powered for the total trial duration because the maximum operating temperature of 120 °C was reached. The Peltier devices had to be deactivated within approximately 1 minute of being powered to prevent any damage occurring to the devices. The Peltier devices remained off for the remainder of the trial, which allowed natural convection to occur until a temperature of 24 °C was reached. In Figure 14, a steeper slope during minute 1 of the trial indicates a more rapid cooling than after the devices are off and natural convection takes over. This can be seen better in the FLIR snapshot, Figure 16, when the devices are powered. The slight square outlines of the Peltier coolers can be seen as the print surface cools. After the Peltier devices are powered off, the temperature of the print surface rises slightly before cooling off. This slight increase in temperature is due to the temperature of the hot side of the Peltier devices bleeding back through the aluminum plate. This temperature rise can be seen by the dramatic increase in the temperature difference at the 1 to 2-minute mark in Figure 15 and in the FLIR snapshot in Figure 17.

Table 5: Heating Average Temperature Comparison

Heating Average Temperature Comparison

Resistance Heating Element Average Temperature					Peltier Heating Average Temperature				
Time (Minutes)	Minimum Temperature (°C)	Average Temperature (°C)	Maximum Temperature (°C)	ΔT (°C)	Time (Minutes)	Minimum Temperature (°C)	Average Temperature (°C)	Maximum Temperature (°C)	ΔT (°C)
0	23.07	23.50	23.87	0.80	0	24.01	24.63	25.09	1.08
1	30.86	38.49	41.79	10.92	1	24.67	30.05	33.66	8.98
2	43.88	54.77	59.75	15.87	2	27.18	34.66	38.13	10.94
3	54.96	66.13	71.41	16.44	3	30.43	38.63	42.12	11.69
4	58.11	66.70	70.47	12.35	4	33.73	42.12	45.69	11.96
					5	36.97	45.29	48.95	11.98
					6	40.57	48.16	51.92	11.35
					7	43.59	50.88	54.81	11.22
					8	45.98	53.45	57.50	11.52
					9	47.81	55.74	59.84	12.03
					10	49.65	57.85	62.03	12.38
					11	51.02	59.77	63.99	12.97
					12	52.63	61.56	66.19	13.56
					13	53.95	63.22	67.80	13.86
					14	55.03	64.68	69.51	14.48
					15	56.22	66.02	71.13	14.91

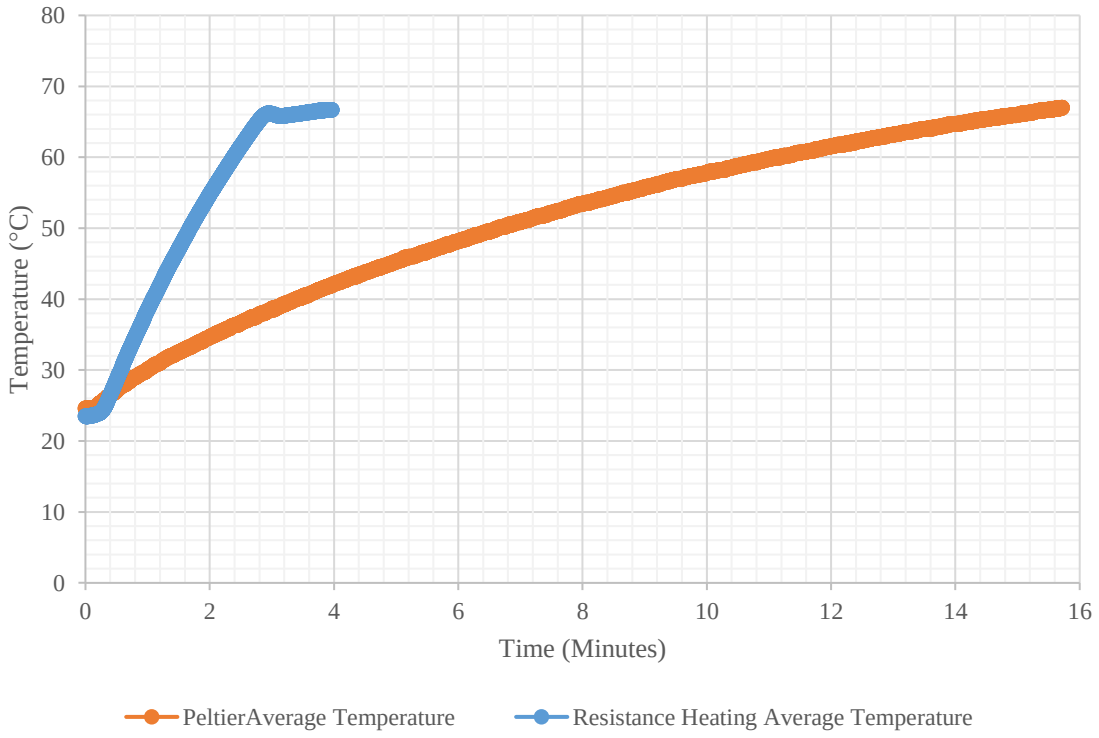

Figure 18: Heating Average Temperature Comparisons

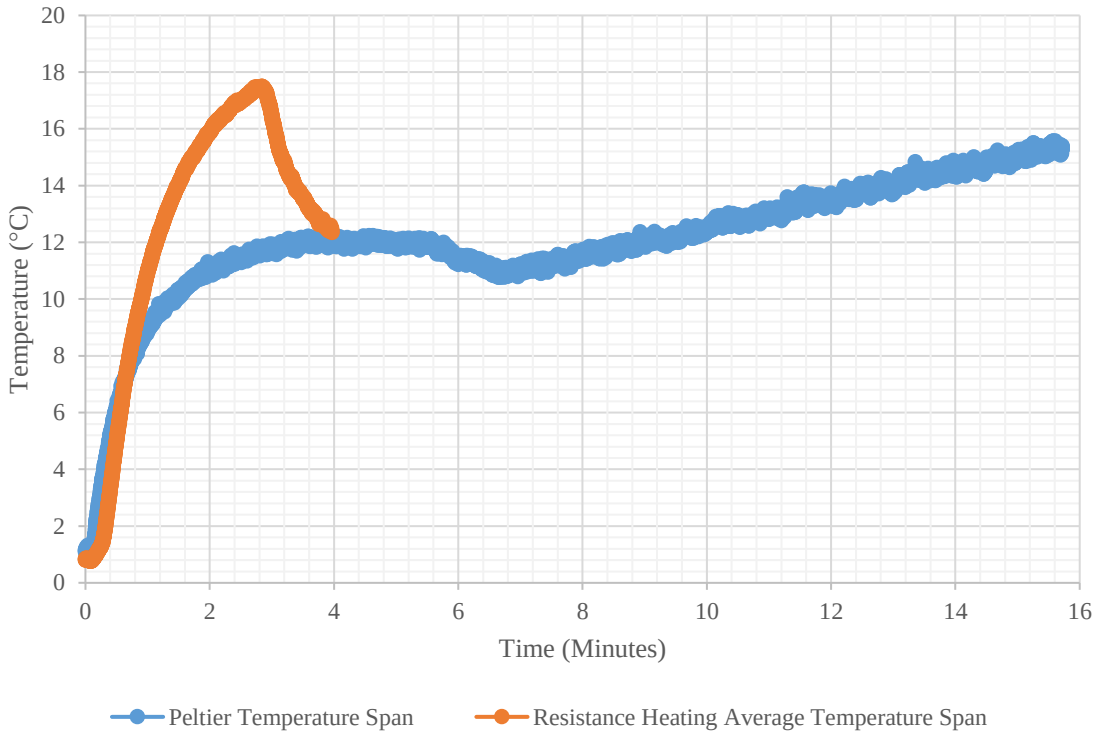

Figure 19: Heating Average Temperature Difference Comparison

Figure 18 shows the average resistance heating and Peltier heating over time. The resistance heating element heated the print bed from 24 °C to 70 °C in 4 minutes, while the Peltier heating took 15.7 minutes. The resistance heating element was nearly 400% faster than the Peltier heating. This large increase in heating time from the Peltier devices significantly increases the cycle time of the printing process, which does not improve manufacturing efficiency. The resistance heating element also was more uniform across the print surface. In Figure 19, the temperature difference for the resistance heater is shown to have a higher value than the Peltier devices. However, when comparing the FLIR snapshots in Figure 7 and Figure 13, the Peltier devices are much less uniform. The higher temperature difference is due to the same issue of the outer edge temperatures of the defined measurement area discussed previously.

Table 6: Cooling Average Temperature Comparison

Cooling Average Temperatures Comparison

Natural Convection Cooling Average Temperature					Peltier Cooling Average Temperature				
Time (Minutes)	Minimum Temperature (°C)	Average Temperature (°C)	Maximum Temperature (°C)	ΔT (°C)	Time (Minutes)	Minimum Temperature (°C)	Average Temperature (°C)	Maximum Temperature (°C)	ΔT (°C)
0	60.45	67.30	70.34	9.89	0	56.59	63.41	65.70	9.12
0.1	60.50	67.35	70.39	9.89	0.1	56.33	62.64	64.88	8.56
0.2	60.42	67.28	70.35	9.94	0.2	56.04	61.80	64.15	8.12
0.3	60.38	67.10	70.12	9.74	0.3	55.81	60.88	63.15	7.34
0.4	60.23	66.75	69.77	9.54	0.4	55.44	60.13	62.23	6.80
0.5	60.14	66.35	69.23	9.10	0.5	54.87	59.45	61.48	6.60
0.6	59.83	65.97	68.76	8.93	0.6	54.53	58.87	60.97	6.45
0.7	59.66	65.57	68.28	8.62	0.7	54.20	58.48	60.70	6.50
0.8	59.49	65.23	67.83	8.34	0.8	53.69	58.06	60.43	6.74
0.9	59.18	64.84	67.40	8.22	0.9	53.25	57.79	60.22	6.97
1.0	58.93	64.50	67.01	8.08	1.0	52.77	57.69	60.18	7.42
1.5	57.71	62.66	64.85	7.14	1.5	51.72	58.06	60.90	9.18
2.0	56.46	60.98	62.95	6.49	2.0	51.32	57.88	60.64	9.32
5.0	49.68	52.66	54.10	4.42	5.0	48.52	52.47	53.84	5.32
10.0	41.85	43.81	44.82	2.97	10.0	39.29	43.05	43.97	4.68
15.0	36.95	38.39	39.20	2.25	15.0	33.44	36.79	37.55	4.11
20.0	33.76	34.85	35.51	1.75	20.0	30.09	32.78	33.42	3.33
25.0	31.48	32.38	32.96	1.49	25.0	27.87	30.05	30.58	2.71
30.0	29.76	30.61	31.18	1.42	30.0	26.60	28.16	28.63	2.03

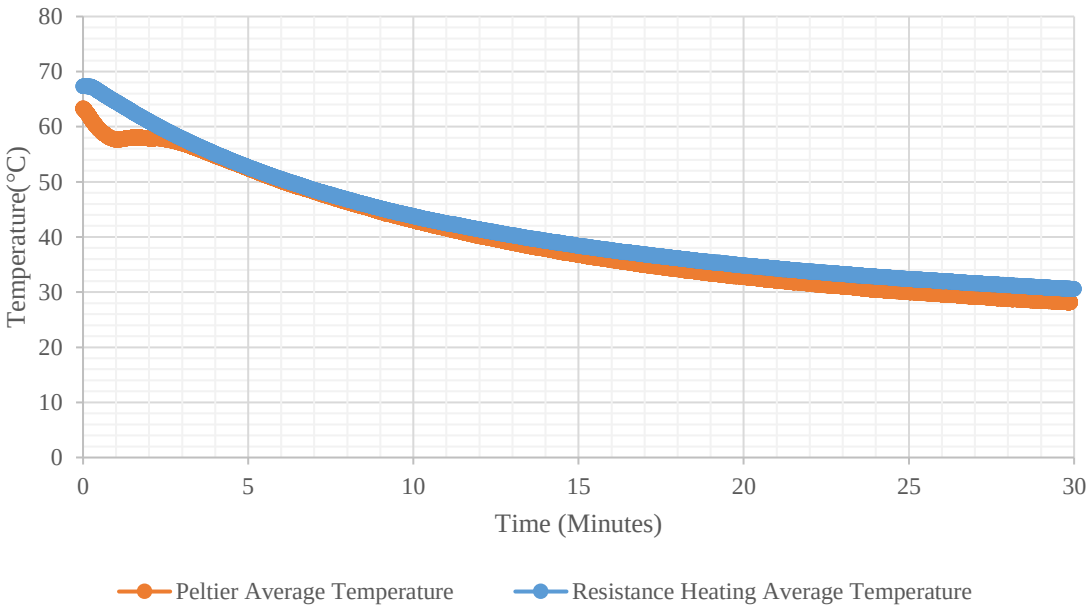

Figure 20: Cooling Average Temperatures Comparison

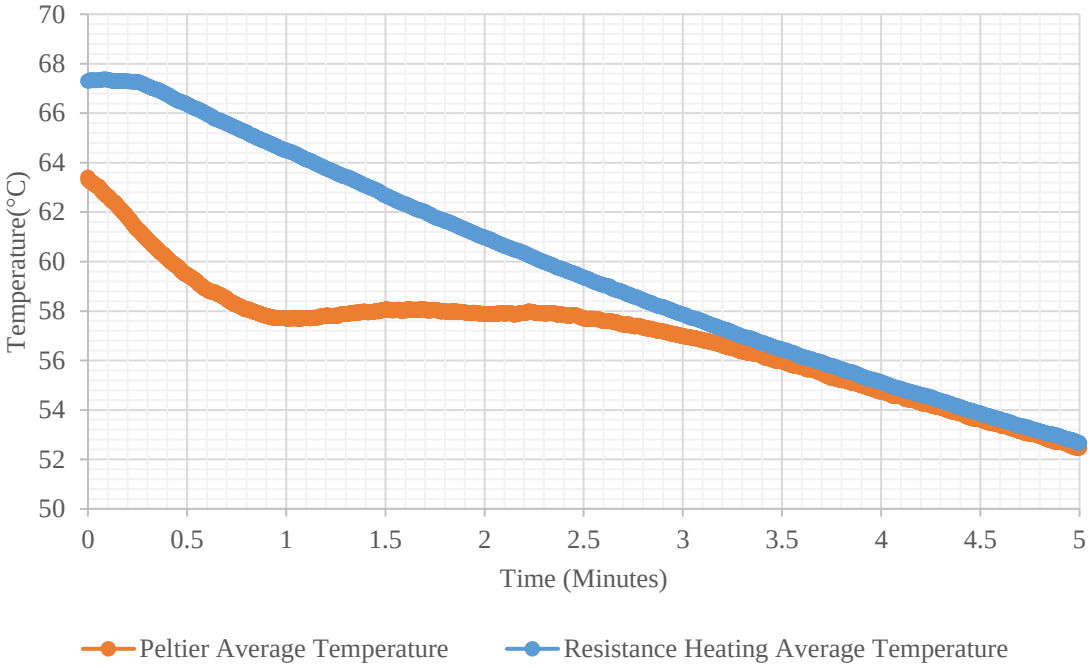

Figure 21: 5 Minute Cooling Average Temperature Comparison

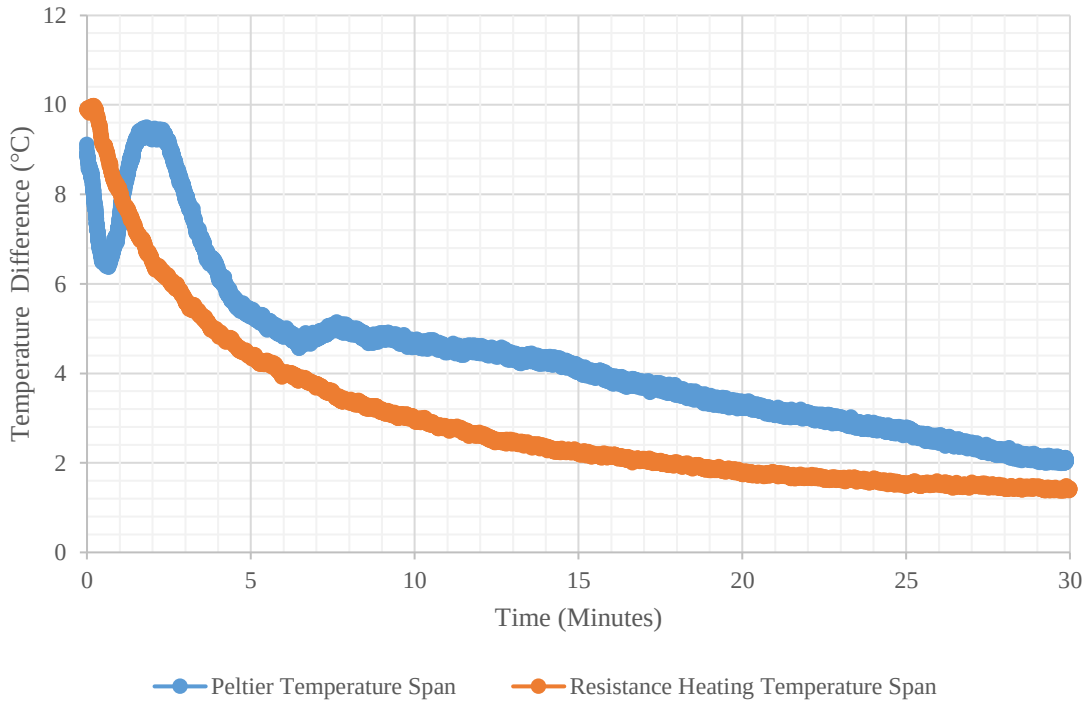

Figure 22: Cooling Average Temperature Difference Comparison

During the first minute of the trial, the Peltier devices were able to cool the print surface more rapidly than natural convection, as indicated by a steeper slope on the curve in Figure 20 and Figure 21. After the first minute, the Peltier devices were powered off due to the maximum operating temperature of 120 °C being reached, and natural convection continued until a temperature of 24 °C. The natural convection curves of both methods closely align. The ΔT across the print surface spikes after the Peltier devices are powered off, as seen in Figure 22. This is due to the heat from the hot side of the Peltier devices bleeding through to the print surface and raising the temperature. This shows the natural convection to be more uniform in cooling the print bed.

4.2 Statistical Analysis

Table 7: Temperature Difference Average and Standard Deviation

	Resistance Heating Element		Peltier Devices	
	Heating	Cooling	Heating	Cooling
Trial	ΔT_{max} (°C)	ΔT_{max} (°C)	ΔT_{max} (°C)	ΔT_{max} (°C)
1	19.13	10.36	15.58	12.01
2	18.16	9.94	16.94	10.65
3	18.42	10.16	17.40	10.05
4	17.73	10.21	15.58	11.10
5	17.93	10.66	16.94	11.50
6	17.71	10.38	17.40	10.72
7	17.49	9.66	16.66	12.86
8	17.15	10.62	21.39	11.72
9	17.60	10.11	17.25	11.90
10	17.42	10.65	17.55	11.25
Average	17.87	10.27	17.27	11.38
σ	0.54	0.31	1.53	0.76

The purpose of statistical analysis is to reveal any random errors within the data set. The standard deviation shows the variability of data distribution. The low standard

deviation values, shown in Table 7, indicate a small deviation from the average and a tight data spread. The standard deviations for the Peltier devices are larger than the resistance heating element, which indicates a more consistent and uniform heating and cooling process for the resistance heating element. This supports the print bed uniformity findings from analyzing the temperature curves and temperature differences in the previous section.

4.3 Experimental Uncertainty

Table 8: List of Equipment Measurement Uncertainties

Measurement/Equipment	Uncertainty
K-type thermocouples	2.2°C
FLIR A300-Series Camera	2°C
Voltage output from power supply	0.01% + 3mV
Current output from power supply	0.1% + 3mA

A list of the equipment used and the range of the uncertainty measurements for each device can be found in Table 7. Additionally, all properties (i.e., ambient temperature, thermal conductivity, emissivity, etc.) were assumed to be constant with zero uncertainty.

6. Conclusion

This project sought to experimentally test a novel idea for an active cooling system for a 3D print bed utilizing Peltier thermoelectric devices in place of the traditional resistance heating element currently used in virtually all existing heated 3D printer beds. The Peltier devices successfully cooled the print bed surface while powered; however, the devices quickly reached the maximum operating temperature and were disabled after the first minute. Extending the operational period would result in an increase of the print bed

cooling and reduce the time taken to reach ambient temperature. The resistance heating element was nearly 400% faster than the Peltier devices while heating the print bed to 70°C. On average, the resistance heater and Peltier devices heated the bed in 4 minutes and 15.7 minutes, respectively. This is a significant issue in terms of reducing the cycle time of the heating and cooling process. The Peltier devices also produced less uniform heating and cooling of the print bed. This is due to, in part, the top row of Peltier devices underperforming compared to the bottom two rows in the 3x3 grid. Provided that each Peltier device performed at the same level, the uniformity across the print surface would still not match the uniformity of the resistance heating element. However, the uniformity of the Peltier devices would more closely resemble the uniformity of the resistance heating element.

In conclusion, this project demonstrated the potential of using Peltier thermoelectric devices as a cooling system for 3D print beds. While the devices showed promising results in rapidly cooling the print bed surface, improvements are needed to extend their operational period and improve the uniformity of heating and cooling across the print surface. Nonetheless, this study provides a foundation for further research and development of more efficient and effective cooling solutions for additive manufacturing.

References

[1] P. B.A, L. N, A. Buradi, S. N, P. B L, and V. R, "A comprehensive review of emerging additive manufacturing (3D printing technology): Methods, materials, applications, challenges, trends and future potential," *Materials Today: Proceedings*, vol. 52, pp. 1309–1313, 2022.

[2] M. Glatt, S. Greco, L. Yi, B. Kirsch, and J. C. Aurich, "Development and implementation of a system for the automated removal of parts produced by fused deposition modeling," *Procedia CIRP*, vol. 103, pp. 109–114, 2021.

[3] S. Sharma, V. K. Dwivedi, and S. N. Pandit, "A review of thermoelectric devices for cooling applications," *International Journal of Green Energy*, vol. 11, no. 9, pp. 899–909, 2014.

[4] M. K. R. Alam, H. Fitriawan, F. X. A. Setyawan, and U. Murdika, Jurnal Teknik Elektro, tech., 2021.

[5] J. Wang, J.-bo Wang, Z.-yi Long, T. Zhu, Z.-sheng Li, Z.-chuan Jiang, and J. Liu, "Design and application of a cooling device based on peltier effect coupled with Electrohydrodynamics," *International Journal of Thermal Sciences*, vol. 162, p. 106761, 2021.

[6] W. H. Phillips, *Additive manufacturing: Opportunities, challenges, implications*. Nova Science Publishers Incorporated, 2016.

[7] E. Pollock, *3D PRINTING: All About the Heat Heating plastic filaments in specialized printers equipped with heated extruders and print beds sets the stage for fused filament fabrication--also known as 3D printing*, vol. 26. BNP Media, 2019.

[8] M. Spoerk, J. Gonzalez-Gutierrez, J. Sapkota, S. Schuschnigg, and C. Holzer, "Effect of the printing bed temperature on the adhesion of parts produced by fused filament fabrication," *Plastics, Rubber and Composites*, vol. 47, no. 1, pp. 17–24, 2017.

[9] M. Barrubeeah, M. Rady, A. Attar, F. Albatati, and A. Abuhabaya, "Design, modeling and parametric optimization of thermoelectric cooling systems for high power density electronic devices," *International Journal of Low-Carbon Technologies*, vol. 16, no. 3, pp. 1060–1076, 2021.

[10] G. Xia, H. Zhao, J. Zhang, H. Yang, B. Feng, Q. Zhang, and X. Song, "Study on performance of the thermoelectric cooling device with novel subchannel Finned Heat Sink," *Energies*, vol. 15, no. 1, p. 145, 2021.

[11] A. Abbas and C.-C. Wang, “Augmentation of natural convection heat sink via using displacement design,” *International Journal of Heat and Mass Transfer*, vol. 154, p. 119757, 2020.

[12] R. Aqeel, A. Raza, S. Ahmed, M. Aashquin, and H. Ali, “Effect of heat sink configuration on the performance of thermoelectric refrigeration,” *2021 IEEE Latin America Electron Devices Conference (LAEDC)*, 2021.

[13] M. Ikeda, T. Nakamura, Y. Kimura, H. Noda, I. Sauciuc, and H. Erturk, “Thermal performance of thermoelectric cooler (TEC) integrated heat sink and optimizing structure for low acoustic noise / power consumption,” *Twenty-Second Annual IEEE Semiconductor Thermal Measurement And Management Symposium*, 2006.